Journal of Marine Research, 44, 473–493, 1986

The meteorologically driven circulation in mid-Chesapeake Bay

by Mário E. C. Vieira[1]

ABSTRACT

Utilizing 20 days of sea level elevation and current records in mid-Chesapeake Bay, the frequency structure of the meteorological forcing is investigated. For periods longer than 8 days the residual sea level inside the Bay is coupled to the coastal elevation forced by the onshore-offshore component of the wind, while at the 3–8 day scale the system was driven by the local longitudinal wind component. It is suggested, however, that the partition of energy between the longitudinal and lateral wind components may determine whether the Bay responds locally to the wind or to the coastal elevations. The 2–2.5 day sea level oscillations could not be identified with a seiche in the Bay; their source is not clear, but the atmospheric pressure is a possibility.

The vertical structure of the residual currents through two cross-sections shows that the layers in the upper 8 m are directly driven by the wind, while in the deeper layers the flow is opposite the wind as a result of the surface slope associated with it. The lag in this counter flow increases from the bottom up and is explained in terms of the phase lag of the surface slope response to the wind and the depth dependence of the current response to the wind.

1. Introduction

The importance of the wind in forcing the subtidal circulation in an estuary has been well documented in the past 10 years. Weisberg (1976) clearly correlated the bottom flow in the Providence River with the local longitudinal wind. The investigations of Elliott and Hendrix (1976) and Elliott (1978) in the Potomac River concluded that the oscillations observed with a period of 2–5 days were due in almost equal parts, to the local wind forcing and the interacting effects from the Bay.

A series of papers (Wang and Elliott, 1978; Elliott and Wang, 1978; Wang 1979b) brought important contributions to the understanding of the meteorologically induced subtidal circulation in the Chesapeake Bay. They found fluctuations of the subtidal sea level in the Bay ranging from 2.5 to 20 days. The 20-day oscillations were related to the Ekman dynamics of the alongshore coastal winds, while the 5-day fluctuations were due to both local wind Ekman forcing and nonlocal coastal effects. The suggestion was made that the 2.5-day oscillations might be the result of a longitudinal seiche in the

1. Marine Sciences Research Center, State University of New York, Stony Brook, New York, 11794, U.S.A.

Bay caused by local winds. In a related study Wang (1979a) reported that the Bay was coupled to the coastal surface elevations, at periods longer than 10 days, as a barotropic response to cross-shore winds.

On the other hand in a study of a region in the middle reaches of the Chesapeake Bay, Pritchard and Rives (1979) observed that the subtidal nongravitational currents in the upper part of the water column were wind driven, while the deeper layers were seen to flow in the opposite direction, but in such a way that the response to the wind started at the bottom and propagated upward. Similar observations were made in the upper Chesapeake Bay (Grano and Pritchard, 1981). Wang (1979b) reported a barotropic (depth independent) flow regime in the lower Bay and a baroclinic (depth dependent) response in the upper Bay, relating them to two forcing mechanisms: the surface slope of the water and the wind stress. He offered a conceptual frictional model which reproduced the observed features and showed the deeper residual currents leading the upper currents and the wind. In a study dealing with the computation of subtidal volume fluxes in mid-Chesapeake Bay, Vieira (1985) suggested that the local axial wind stress drove the upper layers of water while the surface slope drove the middle and bottom layers in the opposite direction.

Still, the influence of the near field and far field wind on the vertical structure of the response of the subtidal estuarine circulation is not well determined. Intensive, site-specific measurements can contribute, however, to a better understanding of the meteorological forcing.

This paper results from a study conducted in the middle reaches of the Chesapeake Bay in October 1977. Its objectives are to investigate the response of a segment in mid-Bay to the meteorological forcing and to determine the mechanism leading to the observed upward progression of the subtidal current.

2. The frequency structure of the meteorological forcing

The data set utilized in this study has been described in detail (Vieira, 1983); it consists of current, tidal elevation and wind records taken in the middle reaches of the Chesapeake Bay (Fig. 1) and is only very briefly outlined here. Records were retrieved from 18 current meters deployed from 12 October to 2 November 1977 in 8 vertical moorings. Eleven of these instruments were deployed on 5 vertical moorings across section G (maximum depth 25 m) and 7 on 3 similar moorings along section H (maximum depth 32 m). Depending on depth, between 1 and 4 current meters were buoyantly suspended in the water column; the instruments utilized were Endeco 105 and 174 (propeller speed sensor) and Braincon 1381 and Aanderaa RCM5 (Savonius rotor). The latter were installed at the bottom of the moorings to minimize surface wave and mooring motion contamination. The current data were resolved about longitudinal and transversal coordinates; for this study, only the longitudinal component was used. The records were low-pass filtered to remove the astronomical tidal

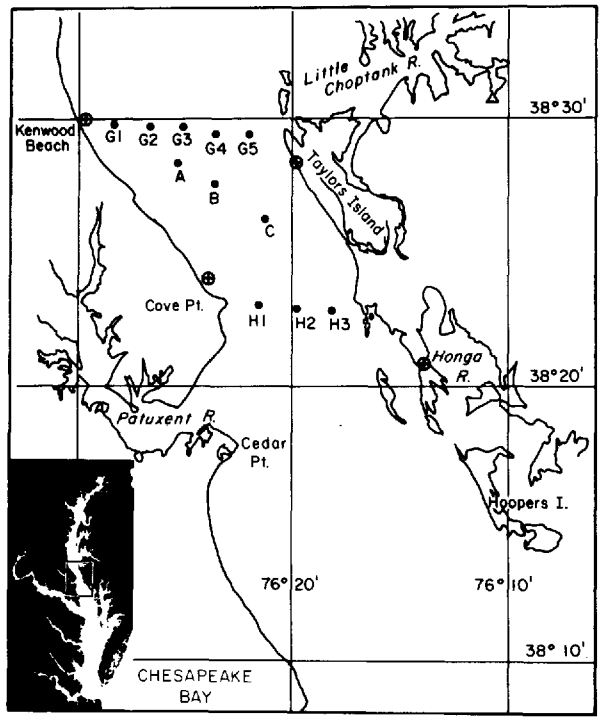

Figure 1. Area of study and position of current meter moorings ● and tide gauges ⊕.

components and higher frequency oscillations (half power point of the filter was 34 hours); the resulting subtidal current records from the 18 instruments deployed in the 2 cross-sections were used with an interpolation scheme to produce laterally averaged longitudinal velocity components at 1 m depth intervals at each section, at 3 hour intervals over the 15 day useful record length. The details of this interpolation/extrapolation scheme are given by Vieira (1985); basically, cubic splines were used to interpolate vertically and horizontally between instruments while extrapolations to the surface, bottom and sides were duly carried out. Figures 2a–d show the lateral mean subtidal flow in cross-section G for the period 16–30 October 1977 at four different depths.

Four temporary tide gauges were installed at the corners of the study area (Fig. 1); in addition sea levels were obtained from NOAA at Annapolis, Solomons Island and Kiptopeake. Figure 3b shows the time series of subtidal sea elevation at Honga River (chosen as representative of the highly coherent surface elevations in the study area) after being subjected to the low-pass filtration described above. The power spectrum of the Honga River subtidal record from 23 September to 25 November 1977 (Fig. 4) is red, pointing out the overwhelming presence of long period fluctuations, i.e., longer

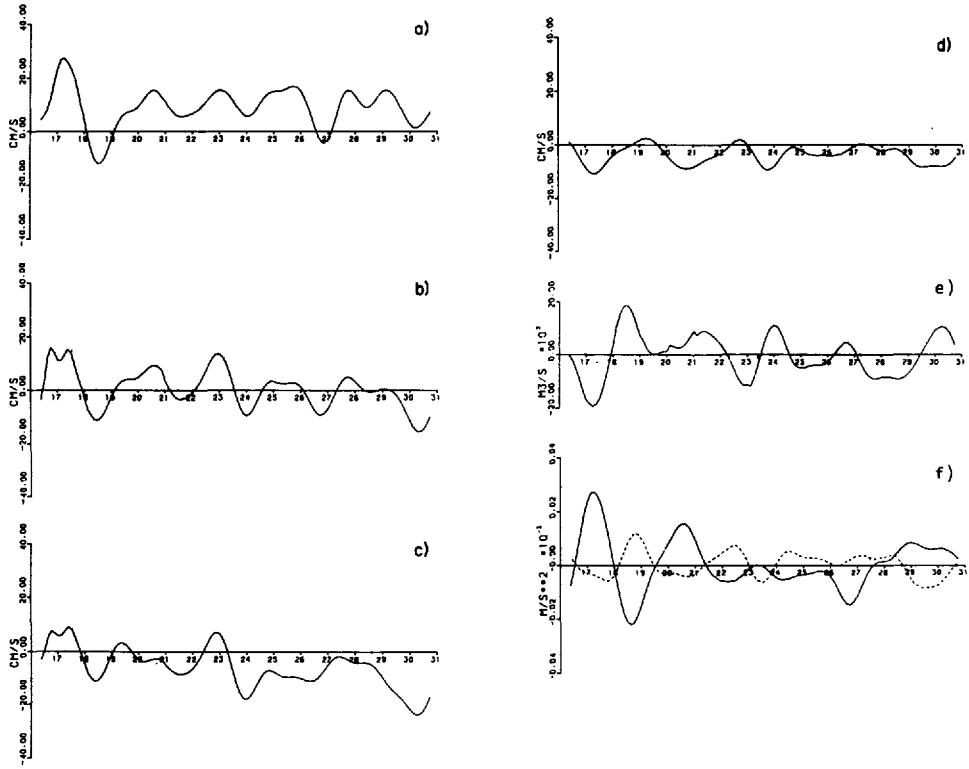

Figure 2. The lateral mean subtidal flow (positive down-estuary) in cross-section G, for the period 16–30 October 1977: (a) between 3–4 m, (b) between 7–8 m, (c) between 11–12 m, (d) between 19–20 m. (e) Time series of $\partial V_r/\partial t$ above cross-section H. (f) Forcing functions with mean and linear trend removed: Patuxent longitudinal wind stress (solid line) and surface slope between Solomons Is. and Annapolis (dashed line).

than about 8 days. The calculation of the number of degrees of freedom and significance levels cited throughout this paper follows Bloomfield (1976).

The wind data from the Patuxent Naval Air Station have been shown to represent conditions over this area (Elliott *et al.*, 1978). The wind stress was computed using a quadratic law (Halpern, 1976) and a drag coefficient of 2.5×10^{-3}; after the low-pass filtration the stress vector was resolved and the longitudinal component extracted along 320°/140° (the geographical axis of the study area) as depicted in Figure 3a.

Detailed information on the frequency structure of the relationship between the wind stress at Patuxent and the Honga River elevations was obtained from coherence squared considerations. As reported by Wong (1982) coherences between sea level elevations and wind stress yield sharper results when the former are corrected for the inverted barometer effect due to the variations in the atmospheric pressure. This correction was introduced (at the rate of 1 cm per mb) and the computed coherence

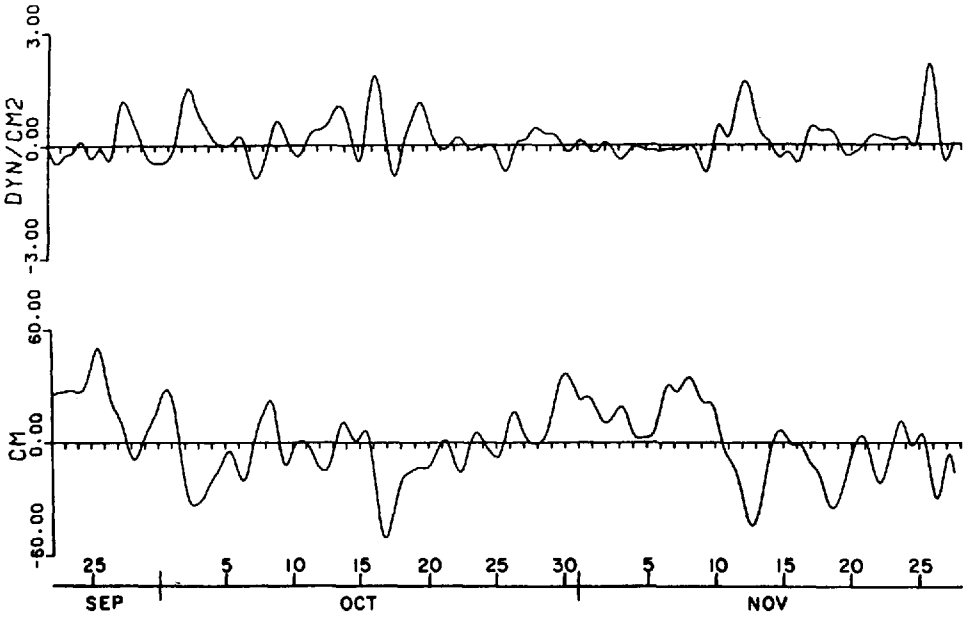

Figure 3. Low-pass time series for 23 Sept.–28 Nov. 1977 of (a) wind stress component along 140°/320° (140° positive), (b) Honga River sea level.

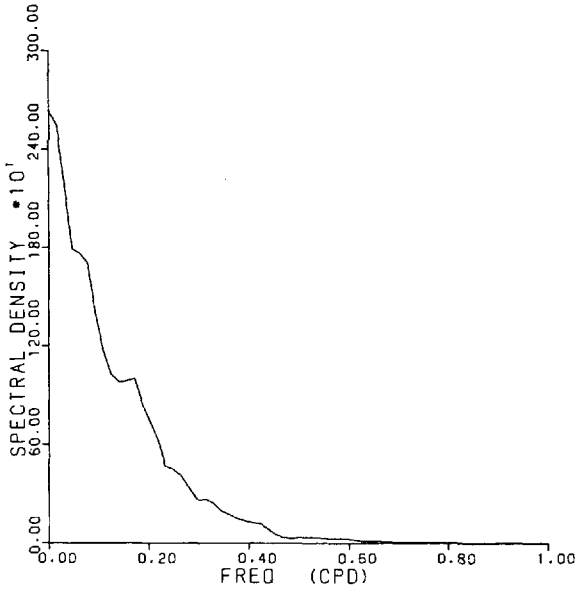

Figure 4. Energy density (cm^2/cpd) spectrum of the Honga River subtidal sea level for the period 23 Sep–25 Nov 1977. Degrees of freedom = 15.3.

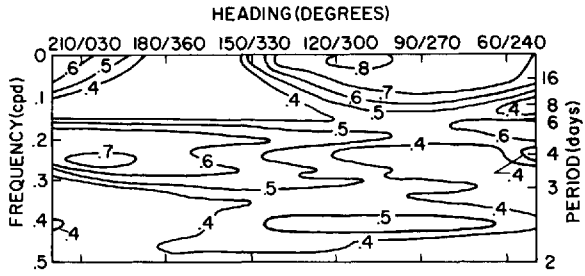

Figure 5. Coherence squared as a function of wind direction between the Patuxent wind stress and the Honga River pressure corrected residual elevations. 95% SL = 0.36.

squared is shown in Figure 5 as a function of frequency and wind direction. Three distinct frequency bands are noted. For periods longer than 8 days the sea level is highly coherent with the E-W component of the wind stress; for periods between 3–8 days it is mostly coherent with the N-S component, while for periods on the order of 2–2.5 days the elevations show a broad band of relatively low coherence, extending over a heading interval of nearly 90° centered in the E-W component.

To investigate the possible effects of the atmospheric pressure upon the water elevation, the coherence squared between the low-passed sea level pressure at Patuxent and the Honga River residual elevation was examined. It was not found to be significant except for periods on the order of 5 and 2–2.7 days when it rises to high values.

In order to interpret these results accessory information must be considered. For periods longer than 8 days the phase difference between the E-W wind stress and the sea level was around 180°, i.e., an eastward wind depressed the surface. However, the power spectrum of $\partial V_\tau/\partial t$ (the time rate of change of the tidally averaged volume of the Bay and tributaries between the head of the tide and cross-section H, Fig. 2e) revealed little energy at these time scales (Fig. 6). Furthermore, the coherence squared between $\partial V_\tau/\partial t$ and the wind stress (Fig. 7) shows practically no relationship between the transport of water and the wind at these frequencies. This suggests that the wind is not directly responsible for the sea level changes, since it produces no transport; the intermediary mechanism might be that variations in the coastal sea level cause fluctuations within the Bay. A computation of the coherence squared between the residual Honga River elevations and those at Kiptopeake (from a gauge near the mouth of the Bay and representative of the coastal elevation) is shown in Figure 8a, revealing their high coherence for periods larger than 8 days with almost no phase lag (Fig. 8b). The conclusion is that for periods larger than 8 days the residual sea level inside the Bay is coupled to the coastal elevations forced by the E-W (or onshore/offshore) component of the wind stress. This is consistent with Wang's study (1979a) of the atmospheric forcing in the Chesapeake Bay, in which the long period fluctuations were seen to result from the barotropic response to the cross-shore wind.

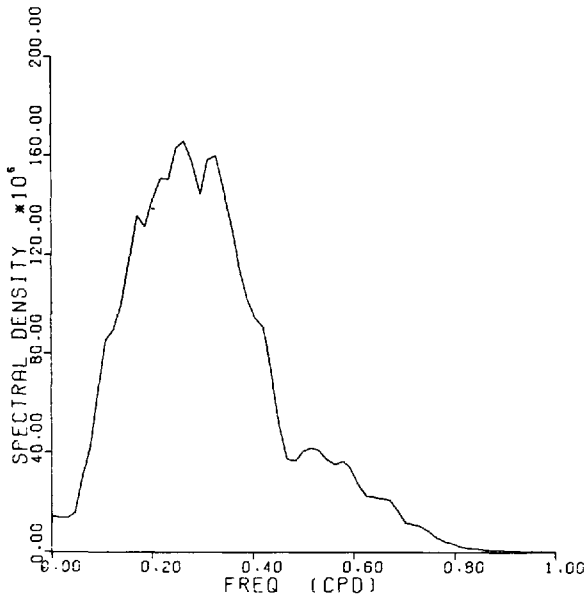

Figure 6. Energy density $[(m^3s^{-1})^2/cpd]$ spectrum of $\partial V_\tau/\partial t$ above cross-section H for the period 23 Sep–25 Nov 1977. Degrees of freedom = 15.3.

At time scales between 3 and 8 days the coherence squared between the Honga River residual elevation and the wind stress shows a maximum for wind headings around 200° (Fig. 5) with phase differences near 180°. This might seem to indicate that a southward wind drives water out of the Bay and a northward wind tends to fill it. However, the coherence squared between the volume flux $\partial V_\tau/\partial t$ and the wind stress (Fig. 7) also shows a maximum centered at about 170°, while the corresponding transfer function shows the wind leading the flux by close to 90°, i.e., winds blowing down-Bay are associated with a transport up-Bay and winds blowing up-Bay are related to a flux down-Bay. These results can be interpreted as follows: first the N-S

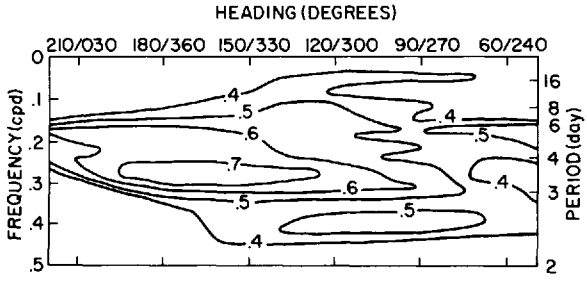

Figure 7. Coherence squared as a function of wind direction between the Patuxent wind stress and $\partial V_\tau/\partial t$ above cross-section H. 95% SL = 0.36.

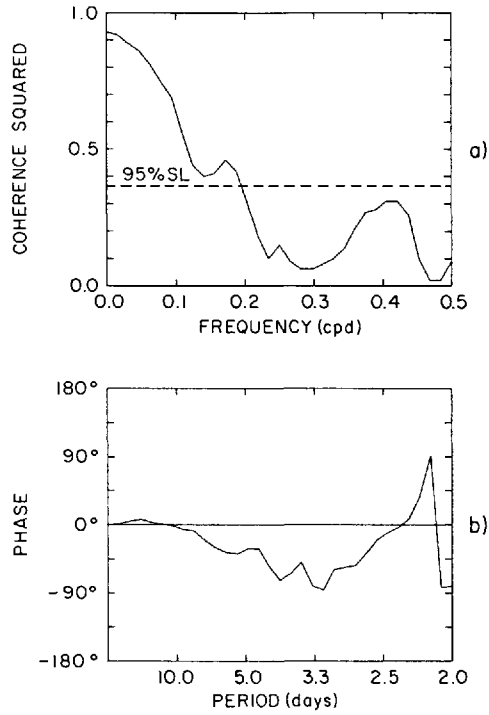

Figure 8. Coherence squared (a) and phase (b) between the residual elevations at Kiptopeake and Honga River. Phase is negative when Kiptopeake leads. The 95% significance level is indicated.

wind component sets up a surface slope in the direction in which it blows; next, this slope induces a barotropic counter flux directed opposite to the wind. For this to be true a reasonable coherence must exist between the N-S wind stress and the longitudinal surface slope on one hand, and between this slope and the volume flux on the other. Indeed, the coherence squared between the Patuxent wind stress and the surface slope (computed as the difference between the Solomons Island and Annapolis residual surface elevations) shows the highest values for headings centered at about 180° (Fig. 9) along with a very slight wind lead. Furthermore the volume flux was coherent with the surface slope at these time scales (Fig. 10) with the slope leading by about 90° (i.e., a positive slope is associated with an inflow of water). Supporting evidence for this interpretation is provided by the high energy contained in the spectrum of $\partial V_r/\partial t$ (Fig. 6) at periods of 3–4 days, as opposed to the little energy displayed by the residual sea level at Honga River for these time scales (Fig. 4). Also note the lack of significant coherence between the sea levels at Honga and Kiptopeake (Fig. 8a) for periods smaller than about 5 days, suggesting no coupling between the Bay and coastal sea levels. It is concluded that at time scales of 3–8 days the residual sea level in the Bay is

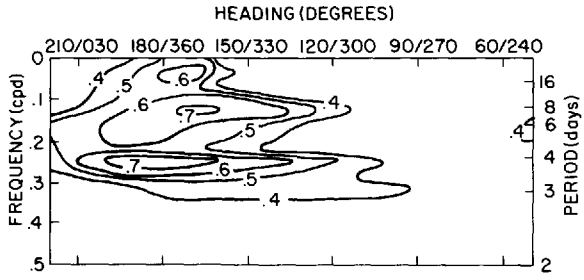

Figure 9. Coherence squared as a function of wind direction between the Patuxent wind stress and the surface slope between Solomons Is. and Annapolis. 95% SL = 0.36.

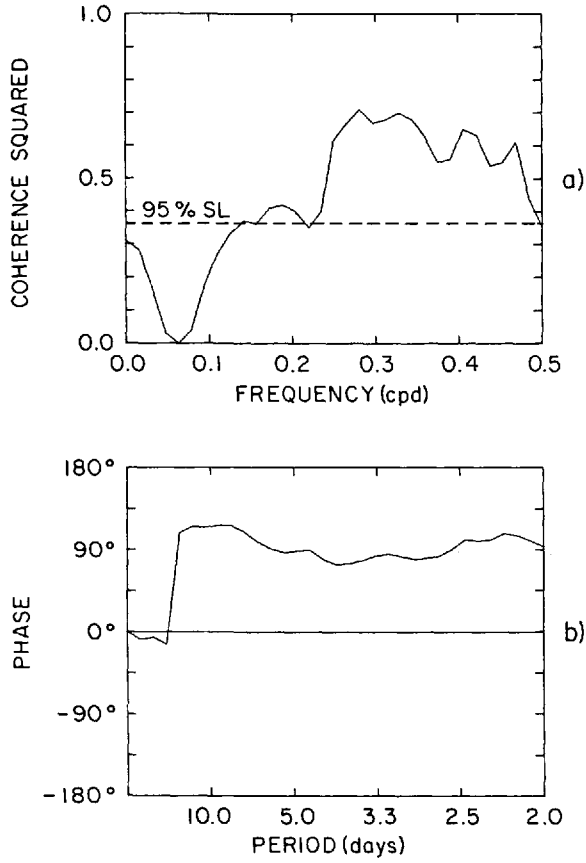

Figure 10. Coherence squared (a) and phase (b) between $\partial V_\tau/\partial t$ above cross-section H and the surface slope between Solomons Is. and Annapolis. Phase is negative when $\partial V_\tau/\partial t$ leads. The 95% significance level is indicated.

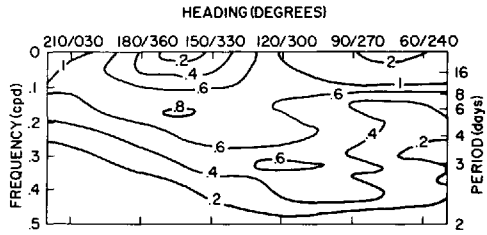

Figure 11. The directional distribution of the spectral energy density [(dyn cm^{-2})^2/cpd] of the Patuxent wind stress.

induced mostly by the local longitudinal wind. In contrast to this, Wang (1979a) found that at these same time scales the elevations in the Bay were coupled to the coastal sea level through an Ekman flow associated with the lateral wind component. However, as the directional distribution of the Patuxent wind stress spectral energy shows (Fig. 11), the most energetic oscillations at these time scales were close to the N-S direction. During Wang's study, on the other hand, these time scales displayed more energy along the E-W direction, which he reasoned being a more effective heading for forcing inside the Bay. This difference in wind energy directional distribution seems, therefore, to be responsible for determining whether the Bay responds to coastal sea levels or to the local wind at these frequencies.

The 2.5 day sea level oscillations show a modest coherence with wind stresses centered at about 100° (Fig. 5), and similarly for the coherence between the volume flux and the wind stress (Fig. 7). However, there is no significant coherence between sea levels at Honga River and Kiptopeake (Fig. 8a) at this time scale, nor is there significant coherence between wind stress and longitudinal surface slope (Fig. 9). These observations seem to preclude a significant relationship between the 2.5 day oscillations on one hand and the local wind or coastal levels on the other. Earlier

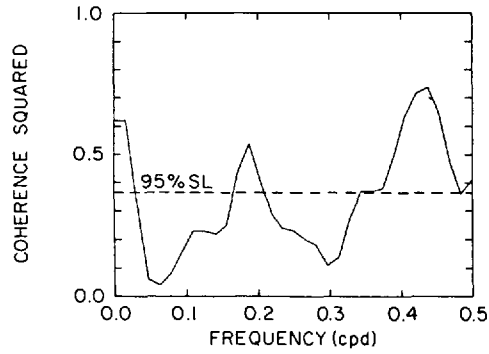

Figure 12. Coherence squared between the sea level pressure at Patuxent and $\partial V_r/\partial t$ above cross-section H. The 95% significance level is indicated.

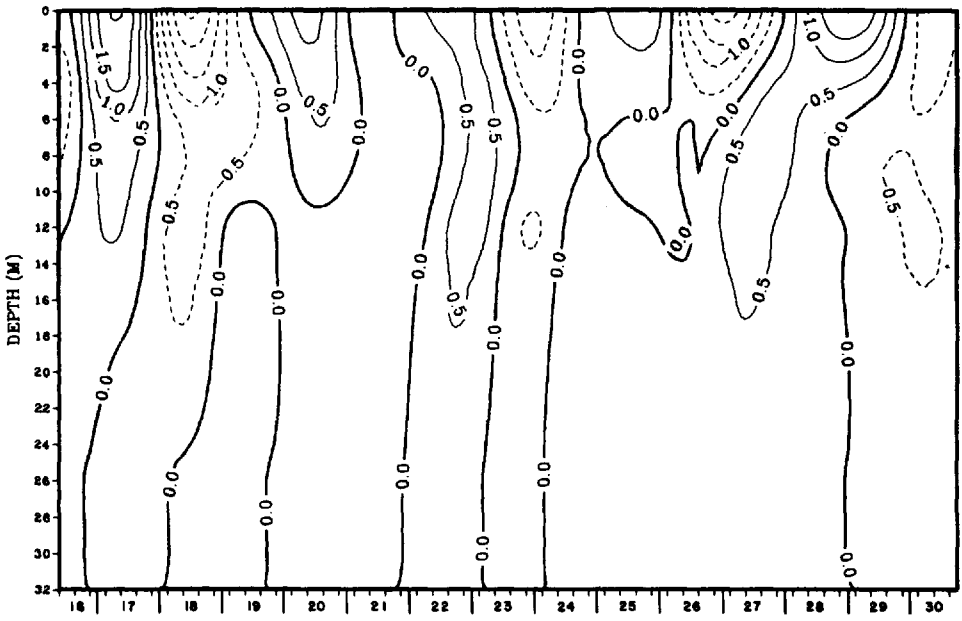

Figure 13. Depth vs. time contours of the laterally integrated subtidal flux per meter of depth at cross-section H. Mean and linear trend removed. Dashed contours indicate landward flux. Units: 10^3 m^2s^{-1}.

investigations (Wang and Elliott, 1978; Elliott and Wang, 1978) have suggested that these oscillations of the sea level inside the Bay constitute a longitudinal seiche caused by the local N-S wind component. However, it is not possible to conciliate the average dimensions of the Bay with even the first mode of free oscillations with a node at the mouth and an antinode at the head. One alternative resides in the atmospheric pressure, which was found to be highly coherent with the Honga River sea level between 2–2.7 days. The suggestion of the possible importance of the atmospheric pressure in driving the 2–2.5 day sea level oscillations is supported by the high coherence squared between the pressure and the volume flux at these scales (Fig. 12).

3. The vertical structure of the flow response

In order to investigate the vertical structure of the residual currents through the cross-sections and their relationship to the forcing functions, the laterally integrated residual mean flows for each 1 m deep layer were utilized. The determination of these residual currents has been previously described by Vieira (1983) who also presents the argument that the density driven motions and those associated with nonlinear interactions can be substantially reduced by removing the mean and linear trend from the current records. This follows from the realization that the residual flows resulting from the nonlinear coupling of tidal oscillations vary only slowly with time, i.e., at

Table 1. Correlation coefficients and lag in hours (in parenthesis) between the lateral mean residual flows for layers 4, 8, 12 and 20. The lag is positive when the column leads the row.

		Layer		
		4	8	12
Layer	8	.79 (−1)		
	12	−.51 (24)	.86 (−3)	
	20	−.58 (9)	−.55 (18)	.48 (−9)

fortnightly and longer periods. Furthermore, the variations in the density distribution (and hence in the gravitational flow) are predominantly of lower frequency than those derived from the meteorological processes due to the wind and atmospheric pressure gradients. Those demeaned and detrended current records can thus be assumed to represent the meteorologically driven motion. Figure 13 shows the time history of the vertical structure of the residual flux through cross-section H during the period 16–30 October 1977.

A lagged correlation analysis was performed, at each cross-section, between the lateral mean residual flows for each meter of depth. Table 1 exemplifies the results at 4 depths in Section G (those from Section H are similar) whose total depth was 25 m (Fig. 2a–d). It indicates that the upper layers lead a reverse flow in the lower layers, this lead decreasing as the bottom is approached. In other words, the flows below about 8 m are reversed in relation to the flows in the upper region and lag them by a decreasing amount as the bottom is approached. This is the upward progression of the residual current response observed by Pritchard and Rives (1979) and discussed by Vieira (1985).

The shape of the power spectra was similar at all depths, as typified by the spectrum at 4 m (Fig. 14), with a peak at about 3 days and most power contained in the band 2–10 days. The energy content of the flow decreased monotonically with depth.

A cross-spectral analysis was also performed between the layers. The results are depicted in Figures 15–17, for the same depths. Layers 20 and 4 are just significantly coherent in the frequency band 0.2 cpd (5 days) to 0.4 cpd (2.5 days). The phase diagram indicates that layer 20 leads layer 4 by about 130° in this frequency interval, corresponding to about 43 hours lead at the 5 d scale and 22 h lead at the 2.5 d. This is not consistent, however, with the correlation results of Table 1. A different interpretation of the phase shift, though, will match the observed correlation and will be physically understandable. Thus, if for a given frequency the coherence squared indicates signal A leading signal B by an angle θ, it can equally be argued that the two records are negatively correlated at that frequency and that record A lags record B by $180° - \theta$. In the present case this means that layer 20 is inversely related to layer 4 and

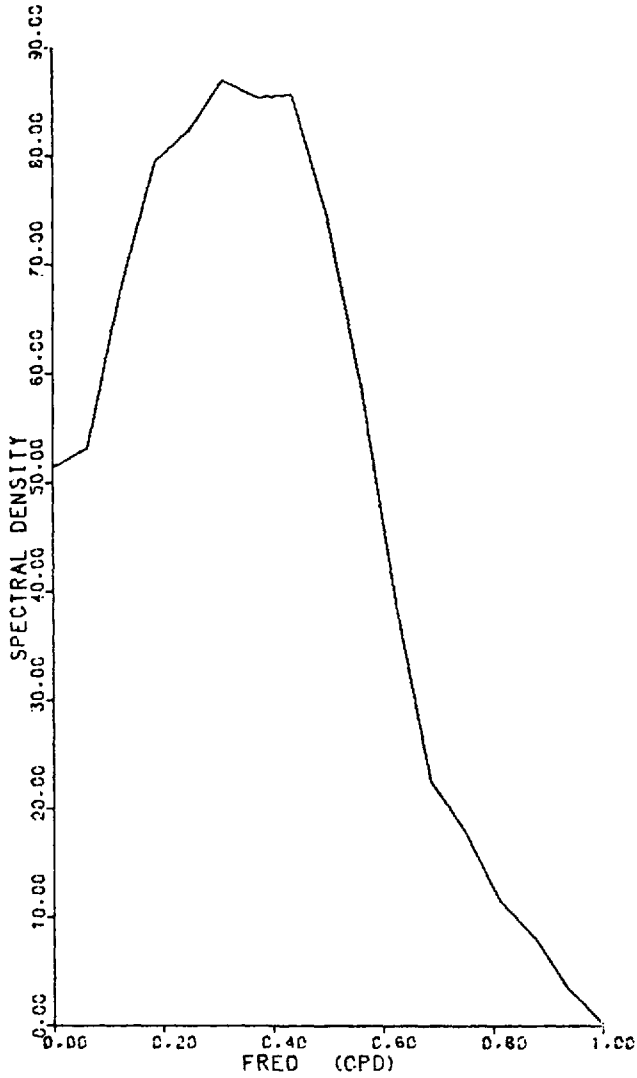

Figure 14. Energy density [(cm s^{-1})^2/cpd] spectrum of the lateral mean residual flow at 4 m in cross-section G between 16–30 October 1977. Degrees of freedom = 13.9.

lags it by about 50°, i.e., 17 h at the 5 d scale and 8 h at 2.5 d. This result is now consistent with the correlation in the time domain (Table 1) which showed a low negative correlation of 0.58 and a 9 h lead by layer 4, keeping in mind the spectral peak at about 3 d.

Similarly Figure 16 shows significant coherence between layers 20 and 8 in the band 2–6.6 d, while the phase can be interpreted as a negative relationship between the

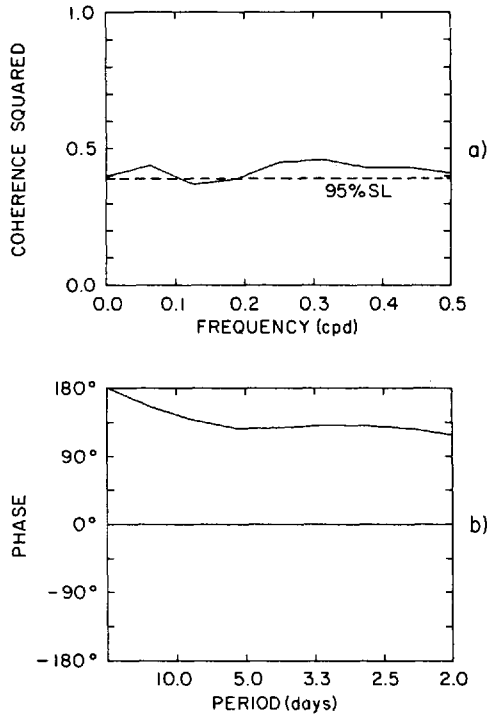

Figure 15. Coherence squared (a) and phase (b) between the lateral mean residual flows at 20 m and 4 m in cross-section G. Phase is positive when flow at 20 m leads. The 95% significance level is indicated.

records with layer 20 lagging layer 8 by 180°–93°, i.e., about 29 h for the 5 d period and 14 h for the 2.5 d period, which again is consistent with the results in Table 1. Figure 17 shows that significant coherence exists between layer 20 and layer 12 over a broad range (2–6.6 d). The phase, however, will match the observed correlations if interpreted directly, that is, layer 20 leading layer 12 by about 52° within that band. This means a positive relationship between layers 20 and 12, with the first leading the latter by 17 h at 5 d and 9 h at 2.5 d. This is not only consistent with the results in Table 1 but also physically plausible, as will be discussed later. It is clear how the sign of the lagged correlation coefficient guides the choice of interpretation of the phase information extracted from the transfer function.

These results indicate that the bottom and middle layers are coherent at periods between 3 and 8 days, with the lower layers leading and the phase propagating upward until about 8 m below the surface; the upper layers, on the other hand, lead the lower layers which flow in the opposite direction. This is consistent with the relationships discussed earlier between the local longitudinal wind stress, the volume flux and the surface slope within this period band.

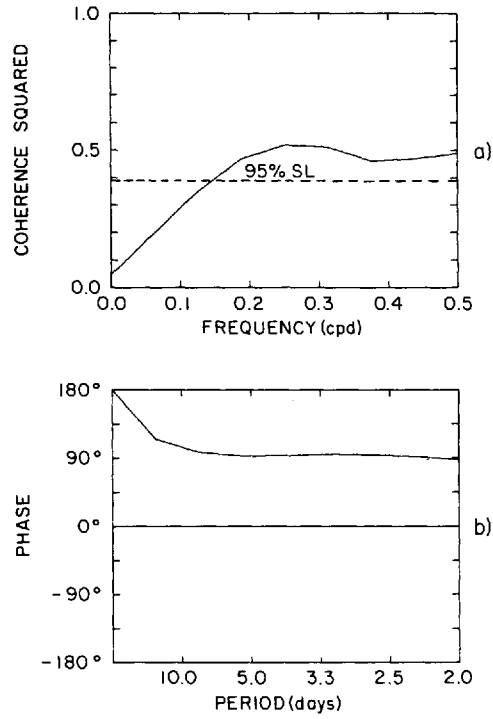

Figure 16. Coherence squared (a) and phase (b) between the lateral mean residual flows at 20 m and 8 m in cross-section G. Phase is positive when flow at 20 m leads. The 95% significance level is indicated.

4. The wind and slope forced residual circulation

The hypothesis of local wind driven surface layers and barotropically forced reverse flow in the middle and lower layers needs to be further investigated. The approach taken involved a cross-spectral analysis directed at examining how each frequency behaved in terms of an independent response to each of the forcing functions.

The problem can be considered as a linear, two parameter input system, where the local axial low-passed wind stress along 320°/140° and the residual surface slope between Solomons Is. and Annapolis are the correlated inputs (recall the high coherences in the band 3–8 days, Fig. 12) and the laterally integrated residual layer mean flow for each 1 m deep layer is the output. The calculations for the transfer function between one of the inputs x_1 and the output y have to allow for a linear least-squares prediction of y from the other input x_2 to be subtracted from y. This concept is applied in the computation of the partial coherence squared between the output and each of the inputs. The procedures utilized are thoroughly discussed in Bendat and Piersol (1971). As mentioned before it was assumed that the contribution from the gravitational circulation was taken out of the time series by removing their

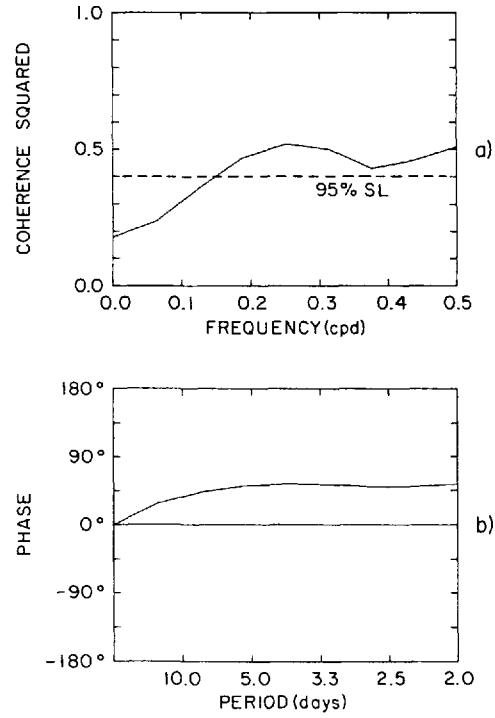

Figure 17. Coherence squared (a) and phase (b) between the lateral mean residual flows at 20 m and 12 m in cross-section G. Phase is positive when flow at 20 m leads. The 95% significance level is indicated.

respective mean and linear trend. The time series of axial wind stress and slope forcing functions are shown in Fig. 2 f with dimensions of acceleration.

Table 2 shows the partial coherence squared between the layer mean flows (only the even numbered depths are presented) and the local axial wind stress as a function of period. Clearly, down to about 8 m deep the currents are significantly coherent with the wind stress for periods up to 8 days; the coherence decreases monotonically with depth, indicating a progressively removed relationship with the wind. Table 2 also lists the phase in hours between the wind and the currents (a minus sign represents a wind lead) corresponding to coherence values above the 95% significance level. It can be seen that the currents lag the wind slightly in the surface layers while there is no appreciable change in phase with depth for a given period. The gain (not shown) between the flow and the wind was found to be approximately uniform with frequency at any given layer, but decreased monotonically with increasing depth, which is consistent with a driving mechanism equally efficient at all frequencies within the band, although progressively less efficient with depth due to internal frictional losses.

The partial coherence squared between the layer mean flows and the surface slope

Table 2. Partial coherence squared and phase in hours (in parenthesis) between the layer mean flows and the axial wind stress with the slope effect removed. Phase negative: wind leads. 95% SL = 0.39.

	PERIOD (Days)			
Layer	8	5.3	4	3.2
2	.44 (−12)	.60 (−8)	.59 (−5)	.65 (−4)
4	.39 (−14)	.54 (−9)	.53 (−6)	.61 (−4)
6	.37	.48 (−9)	.47 (−5)	.55 (−4)
8	.35	.42 (−8)	.39 (−5)	.47 (−4)
10	.28	.31	.28	.30
12	.20	.23	.19	.18
14	.09	.13	.09	.07
16	.04	.07	.03	.02
18	.00	.00	.01	.02
20	.10	.20	.29	.32
22	.13	.27	.34	.38
24	.15	.28	.34	.37

shows significant values at depths below 8 m (Table 3). The phases were consistently above 90° with the currents leading the slope; this was interpreted in the light of the previous discussion, and since one is dealing with sinusoids, as a positive slope leading a negative flow by the supplement of that angle; these angles were converted into hours and are displayed in Table 3 for coherences above the 95% significance level. Thus, within the significant coherence region, the slope leads the flow in the opposite direction by 7 to 15 h, increasing monotonically with decreasing depth, while for any layer this lead is a very weak function of frequency. The gain featured a very slow

Table 3. Partial coherence squared and phase in hours (in parenthesis) between the layer mean flows and the slope with the axial wind stress effect removed. Phase positive: slope leads the flow in the opposite direction. 95% SL = 0.39.

	PERIOD (Days)			
Layer	8	5.3	4	3.2
2	.23	.35	.29	.29
4	.21	.31	.25	.26
6	.24	.32	.28	.30
8	.32	.39 (20)	.37	.42 (14)
10	.32	.38	.39 (14)	.44 (12)
12	.30	.37	.40 (14)	.43 (13)
14	.29	.37	.40 (13)	.41 (12)
16	.31	.40 (12)	.41 (12)	.41 (11)
18	.40 (15)	.50 (12)	.52 (11)	.49 (10)
20	.47 (13)	.59 (11)	.60 (10)	.57 (9)
22	.46 (13)	.58 (11)	.58 (10)	.55 (9)
24	.44 (13)	.56 (11)	.55 (10)	.53 (9)

Table 4. Ordinary coherence squared and phase in degrees (in parenthesis) between the layer mean flows and the axial wind stress. Phase positive: wind lags. 95% SL = 0.39

	PERIOD (Days)							
Layer	8		5.3		4		3.2	
2	.39	(−2)	.52	(−1)	.60	(2)	.68	(0)
4	.40	(3)	.53	(3)	.61	(5)	.69	(3)
6	.40	(12)	.51	(11)	.58	(13)	.66	(11)
8	.34	(31)	.43	(28)	.51	(30)	.57	(28)
10	.25	(54)	.36	(50)	.42	(51)	.44	(49)
12	.19	(71)	.32	(65)	.40	(66)	.39	(64)
14	.17	(110)	.28	(90)	.37	(88)	.33	(85)
16	.27	(131)	.33	(109)	.41	(105)	.36	(103)
18	.49	(144)	.52	(128)	.58	(124)	.53	(124)
20	.70	(152)	.73	(143)	.76	(141)	.74	(141)
22	.72	(153)	.76	(144)	.77	(143)	.76	(143)
24	.73	(153)	.76	(144)	.78	(143)	.76	(143)

increase upward from the bottom layers but came close to a depth independent situation in the layers above 18 m, and was again practically independent of frequency at any given layer. These results agree with the hypothesis; in the middle and bottom layers the pressure gradient induced by the surface slope establishes what is essentially a barotropic circulation, although the effects of bottom friction dampen the amplitude of the current fluctuations below about 18 m.

It is interesting to compare these findings with the theoretical results derived from the frictional model offered by Wang (1979b) to explain the response of the Chesapeake Bay to local wind forcing. That model indicates a depth varying response in the upper Bay and a depth independent response in the lower Bay, with the bottom current leading the surface flow by as much as 130° in the upper Bay. The present study took place in an area between those two extremes; a mixed regime is observed, such that the flows are depth varying in the upper wind driven layers and depth independent in the rest of the column. The implication from Wang's study (*op. cit.* Fig. 6b) is that current fluctuations lead wind fluctuations at any depth, while the phase between these fluctuations increased with depth. However, in the light of the discussion in Section 3 above, it is concluded that in the lower half of the water column the wind led a reverse flow by the supplement angle. This simple interpretation of the physics of the process allows the integration of the two conclusions.

This matter is made clearer by computing the ordinary coherence squared and transfer function between the currents and the axial wind stress alone, therefore with no allowance for the effect of the surface slope. The ordinary coherence squared (Table 4) revealed upper layers down to about 10 m and bottom layers from about 18 m down significantly related to the axial wind stress. These results can be interpreted as follows. The upper layers with significant coherence represent an area in the depth-period plane where wind stress and current oscillations are positively

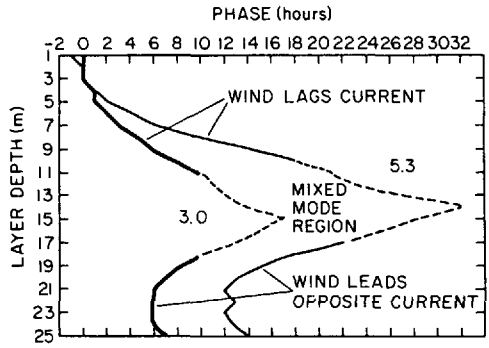

Figure 18. Phase between the wind and the flow at every layer in cross-section G for periods of 5.3 and 3 days.

correlated. The lower layer portion with significant coherence represents negative correlations, where therefore the supplement angle to that listed in Table 4 is the appropriate one. As for the intermediate depth layers with low coherence, they represent a transition zone alternately subjected to a downward movement of characteristics of the upper regime and upward migration of features from the lower regime.

It is helpful to plot the results of Table 4 from this point of view. Figure 18 shows the phase profile (in hours) between the wind and the layer currents at periods of 3.0 and 5.3 days. It is seen that the flow in the upper layers leads the wind increasingly with depth, until the mixed mode region is reached. Keeping in mind that these are harmonic components, this is physically explained as follows. The axial wind stress will tend to drive the surface layers in the same direction with a few hours lag (Table 2); at the same time the water surface is being setup, also with a slight lag, as revealed by the transfer function between the wind stress and the surface slope (not shown). Thus an increased surface flow is being induced opposite to the wind, the balance of the two effects being such that when the wind stress changes sign the surface flow effectively preceded it in the new direction. From Figure 18 it is clear that fluctuations in current lag those of the wind in the bottom layers, this lag increasing with distance upward from the bottom.

5. Discussion

Further insight into the relationship between the meteorological forcing and the residual circulation was obtained. It was concluded that for periods longer than 8 days, the residual sea level inside the Bay is coupled to the coastal elevations forced by the onshore-offshore component of the wind stress. At the 3–8 day scale the local longitudinal wind component drove the system; this contrasts with Wang (1979a) who found the surface elevation at these time scales coupled to the coastal sea level through an Ekman effect due to the lateral wind component. However, the directional

distribution of wind energy during the present experiment favored the N-S direction, whereas during Wang's study it was concentrated mostly along the E-W direction. This suggests that the partition of energy between the longitudinal and lateral components of the wind determines whether the Bay responds locally to the wind or to the coastal elevation. The 2–2.5 day oscillations of the sea level cannot be identified with a seiche in the Bay, as suggested by some investigators. They do not seem related to the local wind nor to the coastal levels. A possibility resides in the effect of the atmospheric pressure. The source of these short-scale oscillations is not clearly understood yet and requires further research.

A linear system was assumed, such that the wind stress and the surface slope are the correlated inputs and the flow at each layer is the output. The analysis of the data shows the direct response of the upper layers (down to about 6–8 m) to the wind stress with some frictional losses but no appreciable phase shift and the response of the middle and bottom layers to the slope with some gain loss and decreasing phase shift as the bottom is approached. Furthermore, a thin mixed response layer was found just below the top wind-driven zone, alternately subjected to the wind-driven and the slope-driven regimes. These findings not only agree with the reported observation of an upward phase propagation of the oscillations in the residual water motion (Wang and Elliott, 1978; Pritchard and Rives, 1979) but also verify the hypothesis advanced by Pritchard and Vieira (1984) of a wind-driven layer in the upper part of the column and barotropic slope driven bottom layers, as a result of the presence of the pycnocline at intermediate depths (7–13 m) which inhibits the downward transfer of momentum from the surface layer and allows the slope term to be dominant over the direct effect of the wind drag.

Acknowledgments. I want to thank Dr. Donald W. Pritchard for his guidance and continued interest in this study. This work was partially funded by the Power Plant Siting Program Energy Administration, Department of Natural Resources of the State of Maryland and by a grant to the Marine Sciences Research Center, State University of New York from the National Science Foundation, Physical Oceanography Program. This is contribution number 509 of the Marine Sciences Research Center.

REFERENCES

Bendat, J. S. and A. G. Piersol. 1971. Random Data: Analysis and Measurement Procedures. Wiley-Interscience, NY, 407 pp.

Bloomfield, P. 1976. Fourier Analysis of Time Series: An Introduction. John Wiley and Sons, NY, 258 pp.

Elliott, A. J. 1978. Observations of the meteorologically induced circulation in the Potomac Estuary. Estuar. Coast. Mar. Sci., *6,* 285–299.

Elliott, A. J. and T. E. Hendrix. 1976. Intensive observations of the circulation in the Potomac Estuary. Chesapeake Bay Institute, The Johns Hopkins University, Spec. Rept. #55, 35 pp.

Elliott, A. J. and D-P. Wang. 1978. The effect of meteorological forcing on the Chesapeake Bay: the coupling between an estuarine system and its adjacent coastal waters, *in* Hydrodynamics

of Estuaries and Fjords, J. C. J. Nihoul, ed., Elsevier Scientific Publishing Co., Amsterdam, 127–145.

Elliott, A. J., D-P. Wang and D. W. Pritchard. 1978. The circulation near the head of Chesapeake Bay. J. Mar. Res., *36*, 643–655.

Grano, V. and D. W. Pritchard. 1981. A study of the spatial variations in the non-tidal currents of the upper Chesapeake Bay. Final report to the Power Plant Siting Program Energy Administration, Department of Natural Resources of the State of Maryland.

Halpern, D. 1976. Measurements of near-surface wind stress over an upwelling region near the Oregon Coast. J. Phys. Oceanogr., *6*, 108–112.

Pritchard, D. W. and S. R. Rives. 1979. Physical hydrography and dispersion in a segment of the Chesapeake Bay adjacent to the Calvert Cliffs Nuclear Power Plant. Chesapeake Bay Institute, Spec. Rept. #74.

Pritchard, D. W. and M. E. C. Vieira. 1984. Vertical variations in residual current response to meteorological forcing in the mid-Chesapeake Bay, *in* The Estuary as a Filter, V. Kennedy, ed., Academic Press, NY, 27–65.

Vieira, M. E. C. 1983. A study of the non-tidal circulation in a segment in the middle reaches of the Chesapeake Bay. Ph.D. dissertation, The Johns Hopkins University, Baltimore, MD, 154 pp.

—— 1985. Estimates of subtidal volume flux in mid Chesapeake Bay. Estuar. Coast. Shelf Sci., *21*, 411–427.

Wang, D-P. 1979a. Subtidal sea level variations in the Chesapeake Bay and relations to atmospheric forcing. J. Phys. Oceanogr., *9*, 413–421.

—— 1979b. Wind-driven circulation in the Chesapeake Bay, Winter 1975. J. Phys. Oceanogr., *9*, 564–572.

Wang, D-P. and A. J. Elliott. 1978. Non-tidal variability in the Chesapeake Bay and Potomac River: Evidence for nonlocal forcing. J. Phys. Oceanogr., *8*, 225–232.

Weisberg, R. H. 1976. The non-tidal flow in the Providence River of Narragansett Bay: a stochastic approach to estuarine circulation. J. Phys. Oceanogr., *6*, 721–734.

Wong, K-C. 1982. Subtidal volume exchange and the relationship to atmospheric forcing in Great South Bay, New York. Ph.D. dissertation, State University of New York at Stony Brook, NY, 230 pp.

Received: *10 May, 1985;* revised: *23 May, 1986.*